Thalamocortical rhythms during a vibrotactile detection task

Saskia Haegens[a,b,c], Yuriria Vázquez[d], Antonio Zainos[d], Manuel Alvarez[d], Ole Jensen[c], and Ranulfo Romo[d,e,1]

[a]Department of Psychiatry, Columbia University College of Physicians and Surgeons, New York, NY 10032; [b]Cognitive Neuroscience and Schizophrenia Program, Nathan Kline Institute, Orangeburg, NY 10962; [c]Donders Institute for Brain, Cognition, and Behaviour, Radboud University Nijmegen, 6500HB, Nijmegen, The Netherlands; [d]Instituto de Fisiología Celular-Neurociencias, Universidad Nacional Autónoma de México, 04510 Mexico D.F., Mexico; and [e]El Colegio Nacional, 06020 Mexico D.F., Mexico

Contributed by Ranulfo Romo, March 24, 2014 (sent for review January 29, 2014)

To explore the role of oscillatory dynamics of the somatosensory thalamocortical network in perception and decision making, we recorded the simultaneous neuronal activity in the ventral posterolateral nucleus (VPL) of the somatosensory thalamus and primary somatosensory cortex (S1) in two macaque monkeys performing a vibrotactile detection task. Actively detecting a vibrotactile stimulus and reporting its perception elicited a sustained poststimulus beta power increase in VPL and an alpha power decrease in S1, in both stimulus-present and stimulus-absent trials. These oscillatory dynamics in the somatosensory thalamocortical network depended on the behavioral context: they were stronger for the active detection condition than for a passive stimulation condition. Furthermore, contrasting stimulus-present vs. stimulus-absent responses, we found that poststimulus theta power increased in both VPL and S1, and alpha/beta power decreased in S1, reflecting the monkey's perceptual decision but not the motor response per se. Additionally, higher prestimulus alpha power in S1 correlated with an increased probability of the monkey reporting a stimulus, regardless of the actual presence of a stimulus. Thus, we found task-related modulations in oscillatory activity, not only in the neocortex but also in the thalamus, depending on behavioral context. Furthermore, oscillatory modulations reflected the perceptual decision process and subsequent behavioral response. We conclude that these early sensory regions, in addition to their primary sensory functions, may be actively involved in perceptual decision making.

Presenting a subject with a (weak) sensory stimulus sometimes leads to perception and sometimes not. What exactly determines the detection of a stimulus has been a central question in the study of sensory perception (1). The neural correlates of somatosensory perceptual detection have been studied extensively in both human and nonhuman primates (2–6). Spike recordings in nonhuman primates showed the contribution of a distributed network of sensorimotor regions to somatosensory decision making, including primary and secondary somatosensory cortices and prefrontal, premotor, and motor areas (7, 8). It was suggested that the neuronal correlates of subjective sensory perception progressively build up as information traverses the cortical circuits, gradually transforming the encoded sensory information into a perceptual decision (5, 9). Crucially, a spike firing rate reflecting the decision process has been detected in secondary somatosensory cortex (S2) and frontal areas, but not in the primary somatosensory cortex (S1) (8, 9).

Previous work focused mainly on the role of the sensorimotor cortex, whereas only a few studies explored the role of the somatosensory thalamus. Most thalamic recordings have been either in tissue slices (10, 11) or in anesthetized animals (12, 13). With only a few studies in awake, behaving animals (14, 15), the thalamic contribution to somatosensory detection performance remained largely unknown. We recently conducted an experiment in which we recorded the simultaneous neuronal activity across the ventral posterolateral nucleus (VPL) and S1 in two monkeys (*Macaca mulatta*) performing a vibrotactile detection task (6, 16). These recordings of single-unit activity in VPL of awake, behaving monkeys showed that neural activity in these nuclei reflects stimulus properties but not the animal's percept (6). Similarly, studies in the lateral geniculate nucleus (LGN), the visual equivalent of VPL, found that spike activity reflects retinal input rather than subjective perception (17, 18). Nevertheless, a study in which spikes were recorded in monkey LGN, showed an enhanced response to attended stimuli compared with nonattended stimuli (19).

Although these studies focusing on single-unit spikes led to many important insights, additional understanding of perceptual decision processes may be gained by studying neuronal population dynamics as reflected by the local field potential (LFP). Several studies in humans (using EEG/magnetoencephalography) showed that cortical oscillatory dynamics influence somatosensory detection performance by setting the state of the brain networks involved (20, 21). Importantly, these studies showed that fluctuations in (anticipatory) prestimulus activity in early sensory areas, predominantly in the alpha (8–14 Hz) and beta bands (15–30 Hz), modulate the likelihood of subsequent stimulus detection (2–4, 22–26).

Here, we report on the oscillatory dynamics in the somatosensory thalamocortical network. We studied LFPs that were recorded concurrently in the aforementioned detection experiments (6, 16) and asked how oscillatory activity contributes to perceptual decision making. To assess the context dependency of stimulus processing, we compared active stimulus detection with a passive control condition. This was done by investigating oscillatory activity in the LFPs of VPL and S1 and by exploring the influence of the observed oscillatory dynamics on task performance.

Significance

When a near-threshold sensory stimulus is presented, a sensory percept may or may not be produced. The exact process by which neural activity elicits subjective perception is a long-standing open question. Here, we ask what role brain oscillations in early sensory regions play in this cognitive process, as oscillations are thought to reflect population dynamics, indicative of the state of a brain network. We found task-related modulations in oscillatory activity in both the somatosensory thalamus and primary sensory cortex, which were correlated with the perceptual decision process and subsequent behavioral response. We conclude that these early sensory regions, in addition to their primary sensory functions, may be actively involved in perceptual decision making.

Author contributions: R.R. designed research; Y.V., A.Z., M.A., and R.R. performed research; S.H., Y.V., O.J., and R.R. analyzed data; and S.H., Y.V., O.J., and R.R. wrote the paper.

The authors declare no conflict of interest.

[1]To whom correspondence should be addressed. E-mail: rromo@ifc.unam.mx.

Results

We recorded LFPs from VPL and S1 in two monkeys performing a vibrotactile detection task (Fig. 1). Here, we explored the role of oscillatory activity as a function of stimulus amplitude and task performance.

Behavioral Performance. The mean detection threshold for both monkeys was 8 μm. Overall performance across sessions on the 10-pulse task was 71.3% correct for m26 (SD = 5.4%; n = 42 sessions) with a sensitivity index (d′) of 1.26 and criterion of 0.40, and 67.9% correct for m27 (SD = 8.1%; n = 21) with a d′ of 1.06 and criterion of 0.42. On the one-pulse task, performance was 63.6% correct for m26 (SD = 5.4%, n = 29), with a d′ of 0.76 and criterion of 0.34.

Amplitude Modulation of Stimulus Response. During stimulus presentation, a 20-Hz peak was observed in the power spectra for both VPL and S1 (Fig. 2). This 20-Hz oscillation reflected an evoked response, i.e., locking of the LFPs to the stimulus frequency. To study the modulation of the evoked response by stimulus amplitude, we obtained the mean power at 20 Hz as a function of stimulus-amplitude class and computed the Spearman correlation, for each region and each stimulus set, for both the active and passive conditions. The 20-Hz LFP power was positively modulated as a function of the stimulus amplitude in both regions (Table 1).

To compare the amplitude modulation between the two regions, we used a two-sample permutation test (over recording sites). We computed the difference in relative power between the no-stimulus condition and the highest amplitude class for each recording site. The modulation by the stimulus amplitude was higher in S1 than in VPL ($P < 0.001$).

In a previous report on the same dataset, we observed an amplitude modulation for spike rate and periodicity similar to the one reported here for 20-Hz LFP power, with stronger firing rate modulation in S1 than VPL (16). It is possible that both the LFP response and the changes in spike activity are driven directly by the stimulus; another possibility is that the LFP power modulation at 20 Hz is caused by the modulations in spiking activity. In this regard, note that there are different types of neurons based on their response to stimulation: (*i*) those that increase their firing rate with stimulation, (*ii*) those that keep the same firing rate but synchronize to the stimulus rhythm, and (*iii*) those that combine both these effects. To further assess the nature of the interaction between the spike activity and the LFPs, we computed the spike–field coherence (SFC) between VPL and S1, in both directions (Fig. 2*D*). We found a stronger SFC around 20 Hz for VPL spikes and S1 fields, compared with S1 spikes and VPL fields (cluster-corrected $P < 0.001$), which likely reflects VPL spikes driving S1 LFPs. We then computed the VPL–S1 SFC per amplitude class (Fig. 2 *E* and *F*) and found a strong modulation of 20 Hz SFC by stimulus amplitude ($r = 0.964$, $P < 0.01$, $n = 33$ for set 1; $r = 1$, $P < 0.001$, $n = 26$ for set 2). Significant amplitude modulation also was observed for the S1–VPL SFC ($r = 0.929$, $P < 0.01$, $n = 27$ for set 1; $r = 0.881$, $P < 0.01$, $n = 20$ for set 2).

Task-Related Beta Increase in VPL and Alpha Decrease in S1. To study the dynamics of the oscillatory activity in the LFPs during the task, we calculated the (relative) baseline-corrected time-frequency representations (TFRs) of power (Fig. 3). In VPL, we observed a sustained increase in beta activity during the poststimulus period (i.e., when the animal was waiting to communicate its perceptual decision by button press) compared with baseline, for both the stimulus-present and stimulus-absent trials, comparable in both monkeys (cluster-corrected $P < 0.001$ for m26, Fig. 3*A*, *Left*; $P < 0.05$ for m27, Fig. 3*B*, note an apparent beta frequency increase for m27). In S1, we observed a sustained decrease in alpha activity during the poststimulus period compared with baseline, for both the stimulus-present and stimulus-absent trials (cluster-corrected $P < 0.001$, Fig. 3*A*, *Right*). Furthermore, in both regions, there was a broadband evoked response to the stimulus.

Because the beta increase in VPL was observed in both the stimulus-present and stimulus-absent trials, it is unlikely that it was triggered by the 20-Hz stimulus frequency. However, to discard this possibility completely, we performed the same analysis on the one-pulse experiment in m26 (Fig. 4). This replicated the above-mentioned findings: again, we observed a prominent beta increase in VPL and an alpha decrease in S1 during the task compared with baseline activity (cluster-corrected $P < 0.05$ for all comparisons). Thus, the beta increase was observed in both the 10-pulse and the one-pulse experiment, in the stimulus-present as well as the stimulus-absent trials. Hence, it cannot be related to the frequency or amplitude of stimulation and likely is related to other aspects of the detection task.

To evaluate whether the observed alpha and beta band modulations were task specific, we contrasted the active experimental condition with the passive control condition (Fig. 5). In the passive condition, the animal received the same stimuli and all other trial parameters were the same, but no response was required to obtain a reward (6). Thus, by comparing the stimulus-present trials of the two conditions directly, we could differentiate between passive stimulus processing and active detection. As the control condition contained fewer recording sites and trials, we stratified the sites and trials from the active condition to fully match the controls (i.e., the same number of trials per stimulus-amplitude class). We focused the statistical analysis on

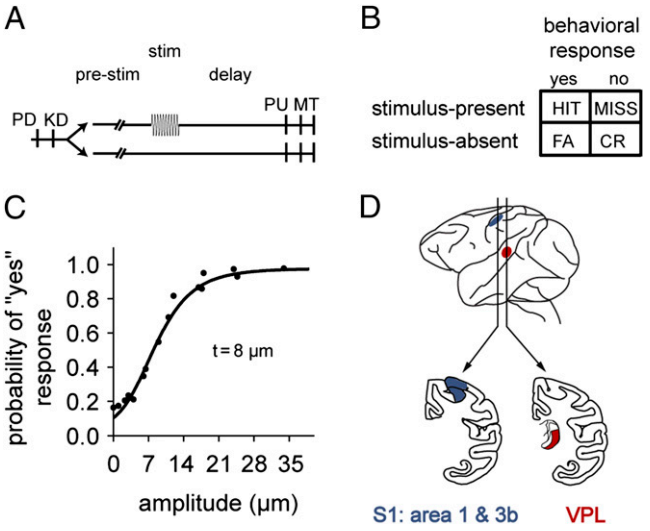

Fig. 1. Somatosensory detection task. (*A*) Trials began with the stimulator probe indenting the skin of one fingertip of the restrained right hand (probe down, PD), upon which the monkey placed its left, free hand on a key (key down, KD). After a variable prestimulus period (1.5–3 s), in half the trials, a vibrotactile stimulus was presented (20 Hz, 0.5 s) with sub- to suprathreshold amplitude (1–34 μm). Stimulus-present and stimulus-absent trials were interleaved randomly. After a fixed delay (3 s for m26, 2 s for m27), the stimulator probe went up (probe up, PU), indicating to the monkey that it could report its perception by pressing one of two buttons with the left hand (response movement, MT). Note that here the 10-pulse task is depicted. (*B*) The detection task elicited four behavioral responses: a hit or miss during stimulus-present trials and correct rejection (CR) or false alarm (FA) during stimulus-absent trials. (*C*) Psychometric function depicting the probability of the monkey reporting that a stimulus was perceived as a function of stimulus amplitude. (*D*) Recording sites: VPL in the somatosensory thalamus and S1.

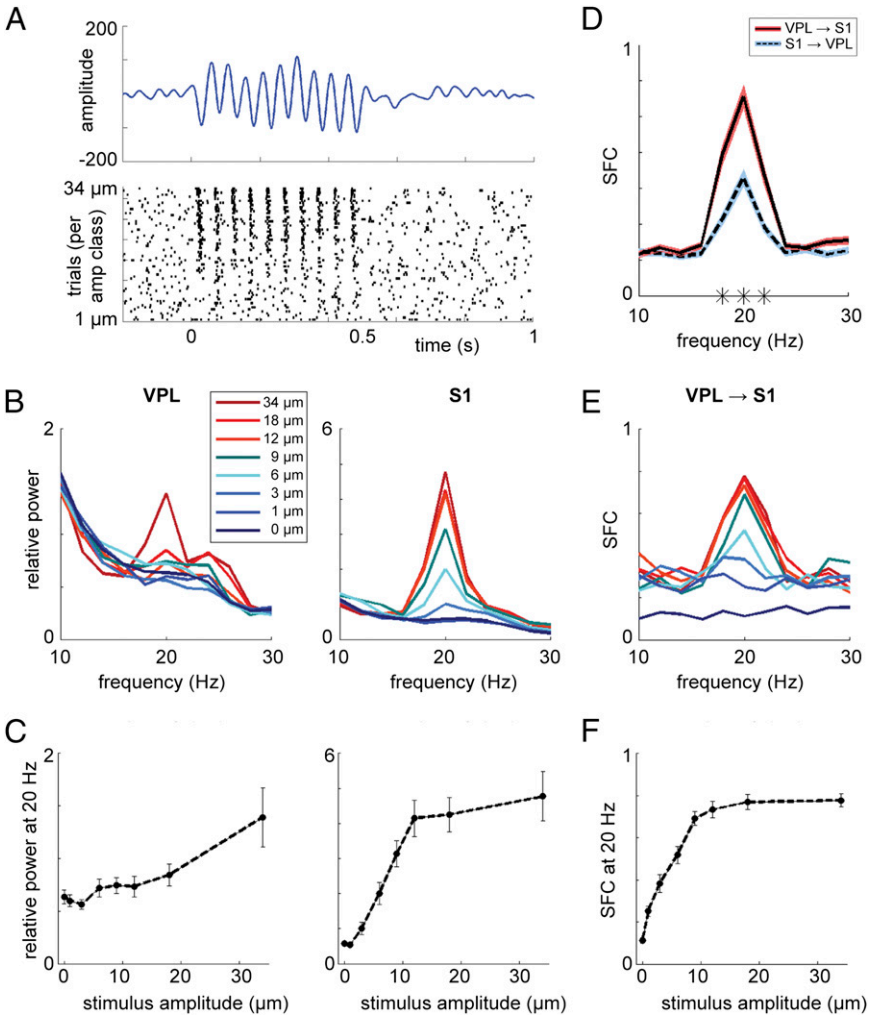

Fig. 2. Amplitude modulation. (*A*, *Upper*) LFP-evoked response for the active stimulus-present trials in one representative recording in S1 in m26. (*Lower*) Spike raster plot for the same recording, plotted per trial, sorted for stimulus amplitude. (*B*) Power spectra during the stimulus window ($t = 0$–0.5 s) averaged over trials per stimulus-amplitude class (showing one subset of stimuli for m26) in VPL (*Left*) and S1 (*Right*). (*C*) Graphs showing positive modulation of 20-Hz power by the stimulus amplitude for both VPL (*Left*; $r = 0.881$, $P < 0.01$) and S1 (*Right*; $r = 0.976$, $P < 0.001$). Error bars indicate the SEM. (*D*) SFC for VPL spikes, S1 fields (red), and S1 spikes, VPL fields (blue), averaged over all stimulus-present trials in the active condition, in m26. A significant difference was observed around the 20-Hz peak for the VPL–S1 vs. S1–VPL SFC (indicated by asterisks; cluster-corrected $P < 0.001$). (*E*) Similar to *B* but showing the SFC for VPL–S1. (*F*) Similar to *C* but showing the SFC for VPL–S1 ($r = 1$, $P < 0.001$).

the time windows in which we observed the sustained alpha/beta effects in the active condition [VPL: from stimulus onset to probe up (PU); S1: from $t = 1.5$ s to PU]. Comparing active vs. passive TFRs showed that the beta increment in VPL was more prominent when the monkey was in a context in which it was forced to actively detect and report the stimulus to receive a reward than when it was just passively stimulated and randomly rewarded (cluster-corrected $P < 0.01$ for both m26 and m27; note the difference in observed beta frequency range between the two animals; Fig. 5 *A* and *B*). Similarly, the S1 decrease in the alpha band for the poststimulus period was stronger for the active than the passive condition (cluster-corrected $P < 0.05$; Fig. 5*A*).

To summarize, actively detecting a stimulus and reporting its perception led to a sustained beta band increase in VPL, whereas in S1, a sustained decrease in alpha was observed. These oscillatory modulations depended on the behavioral context: the modulations were stronger for the active than the passive condition.

Perceptual Decision-Related Oscillatory Modulations in VPL and S1. To assess whether any of the task-related oscillatory activity predicted the monkey's performance and/or decision, we computed behavioral contrasts. There are two possibilities: oscillatory activity might reflect (*i*) behavioral performance, i.e., correct vs. incorrect responses, which would be revealed by the contrast [hits + correct rejections] vs. [misses + false alarms], or (*ii*) decision outcome, i.e., stimulus-present vs. stimulus-absent responses regardless of their accuracy, which would be reflected by the contrast [hits + false alarms] vs. [misses + correct rejections].

Note that for these analyses, we combined the data of both monkeys, and collapsed across the stimulus-present and stimulus-absent conditions, to have enough trials for the behavioral contrasts. Because some sessions contained very few false alarms and/or misses, we included only sessions that had at least 20 trials per contrast of interest (VPL: 38 sites for m26, 20 for m27; S1: 59 sites for m26, 3 for m27). Furthermore, here we did not stratify the data (as we did for the active vs. passive contrast), i.e., hits contained more suprathreshold stimuli than misses, which were limited mostly to subthreshold trials. Given the trial number per stimulus-amplitude class, and the ratio of hits to misses per class, full stratification would have reduced the trial number to such an extent that reliable analysis would not be feasible. Thus, any

Table 1. Amplitude modulation

			VPL			S1		
Monkey	Set	Condition	*r*	*P*	*n*	*r*	*P*	*n*
m26	1	Active task	0.786	<0.05	23	1	<0.001	31
m26	2	Active task	0.881	<0.01	15	0.976	<0.001	28
m27	1	Active task	0.607	0.167	20	0.750	0.066	3
m26	1	Passive control	0.857	<0.05	13	0.964	<0.01	19
m26	2	Passive control	0.810	<0.05	8	0.929	<0.01	16
m27	1	Passive control	0.857	<0.05	11	—	—	—

Power spectra at 20 Hz during the stimulus window (t = 0–0.5 s) were averaged over trials per stimulus-amplitude class. A positive modulation of 20-Hz power by the stimulus amplitude was observed (Spearman correlation).

differences confined to the stimulus window might be the result of (or cannot be distinguished from) stimulus-amplitude differences rather than actual differences in endogenous brain activity.

First, to assess modulation reflecting the monkey's performance, we contrasted correct vs. incorrect responses. This contrast did not yield any significant effects outside the stimulus and immediate poststimulus windows (we ignored this period because it may have been confounded by stimulus-amplitude differences; see above). Thus, the oscillatory activity in VPL and S1 appeared not to be predictive of the monkey's task performance (Fig. 6*A*).

Second, to assess whether oscillatory modulations reflected the monkey's perceptual decision, we contrasted stimulus-present vs. stimulus-absent responses. This contrast did yield significant effects during the delayed response window (cluster-corrected $P < 0.05$; Fig. 6*B*). In both VPL and S1, we observed a significant increase in the theta frequency range that was stronger for stimulus-present responses (hits and false alarms) than for stimulus-absent responses (misses and correct rejections). In S1, we also observed a sustained decrease in alpha/beta activity that was stronger for stimulus-present than for stimulus-absent responses.

Next, to establish whether the observed differences between stimulus-present and stimulus-absent responses reflected the decision outcome, rather than simply the preparation for the upcoming motor response (i.e., left vs. right button press), we analyzed the light control condition. In this condition, animals received the same stimuli, but a light that was on during the entire trial indicated which button was to be pressed. Buttons were assigned regardless of actual stimulus presence. We contrasted control trials with left vs. right button presses (note that the same response hand was used in all trials) and found no sustained differences between the two responses in either VPL or S1 (Fig. 6*C*).

We conclude that the oscillatory modulations observed during the active condition reflect the monkeys' decision outcome. Both in VPL and S1, we observed oscillatory modulations that predicted the monkey's perceptual decision (stimulus present or absent) rather than performance (correct or incorrect) per se. Because no such difference was observed in the motor control condition, the result cannot be explained by simple motor preparation.

Prestimulus Alpha in S1 but Not in VPL Biases Behavioral Response. To address the influence of prestimulus activity on the monkey's behavioral performance, we computed mean alpha power (10–14 Hz) during a 1-s prestimulus window for each trial. Per session, trials were divided (using a median split) in two bins: low vs. high prestimulus alpha power (Fig. 7). This was done separately for stimulus-present and stimulus-absent trials. For each bin, we computed the probability of the monkey giving a "yes" response, indicating stimulus detection (i.e., hits for stimulus-present and false alarms for stimulus-absent trials). Note that for the statistical analysis (paired-samples t test), here we combined the recording sites from both monkeys.

In VPL, no significant difference in behavioral response was observed for low vs. high prestimulus alpha power (Fig. 7*A*) in either the stimulus-present [t (57) = 0.611, uncorrected P = 0.544] or stimulus-absent trials [t (57) = 0.937, uncorrected P = 0.353]. However, in S1, higher prestimulus alpha power led to a small but significant increase in the probability of a yes response (Fig. 7*B*), regardless of actual stimulus presence [t (61) = –2.839, Bonferroni-corrected $P < 0.05$ for stimulus-present trials; t (61) = –3.619, Bonferroni-corrected $P < 0.01$ for stimulus-absent trials]. We then combined all trials (both stimulus-present and -absent), again split

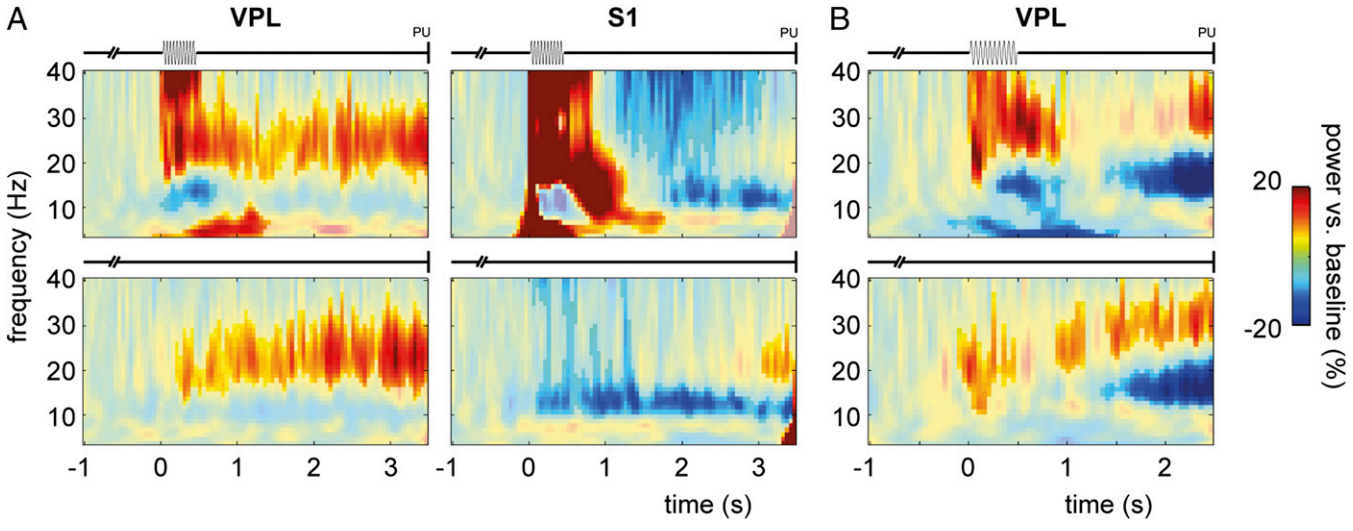

Fig. 3. Oscillatory activity during somatosensory detection task: 10-pulse. (*A*) TFRs of power (4–40 Hz) for stimulus-present trials (*Upper*) and stimulus-absent trials (*Lower*) for VPL (*Left*; averaged over 38 sites) and S1 (*Right*; n = 59 sites) in m26. Power is opacity masked for significant results (cluster-corrected $P <$ 0.05), based on a nonparametric randomization test of task-related activity (stimulus window t = 0–0.5 s and poststimulus window t = 0.5–3.5 s) vs. baseline (t = −1 to −0.5 s). Note that for stimulus-absent trials, t = 0 s is somewhat arbitrary, as it indicates the onset of the stimulus window although no stimulus was presented; however, it makes the TFRs comparable to the stimulus-present case. (*B*) Similar presentation for VPL in m27 (n = 20 sites). Note that for m27, the poststimulus window was shorter (t = 0.5–2.5 s).

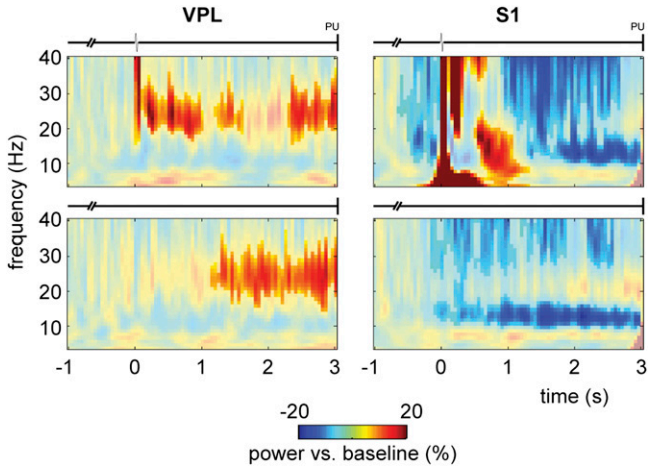

Fig. 4. Oscillatory activity during somatosensory detection task: 1-pulse. TFRs of power (4–40 Hz) for stimulus-present (*Upper*) and stimulus-absent trials (*Lower*) for VPL (*Left*; $n = 26$ sites) and S1 (*Right*; $n = 43$ sites) in m26. Power is masked for significant results (cluster-corrected $P < 0.05$), based on a nonparametric randomization test of task-related activity (stimulus window $t = 0$–0.05 s and poststimulus window $t = 0.05$–3 s) vs. baseline ($t = -1$ to -0.5 s).

them in low and high prestimulus alpha bins, and computed the sensitivity index, d′, and the criterion for signal detection. In VPL, again no significant differences were detected between low and high prestimulus alpha power (Fig. 7*C*) in either d′ [t (57) = 0.260, uncorrected $P = 0.796$] or the criterion [t (57) = −0.297, uncorrected $P = 0.767$]. In S1, higher prestimulus alpha power led to a lower criterion level [t (61) = 3.738, Bonferroni-corrected $P < 0.01$], whereas there was no significant change in d′ [t (61) = 1.726, uncorrected $P = 0.090$], i.e., higher alpha changed the response bias but did not lead to changes in sensitivity (Fig. 7*D*).

These findings were replicated for the one-pulse experiment (Fig. 8): no significant differences were observed in VPL [stimulus-present: t (25) = −1.038, uncorrected $P = 0.309$; stimulus-absent: t (25) = 1.513, uncorrected $P = 0.143$; d′: t (25) = −1.685, uncorrected $P = 0.105$; criterion: $t = -0.415$, uncorrected $P = 0.682$], whereas in S1, higher prestimulus alpha power led to more yes responses in both the stimulus-present [t (42) = −5.611, Bonferroni-corrected $P < 0.001$] and stimulus-absent trials [t (42) = −2.905, Bonferroni-corrected $P < 0.05$], as well as a lower criterion [t (42) = 4.354, Bonferroni-corrected $P < 0.001$], with no difference in d′ [t (42) = −0.539, uncorrected $P = 0.593$].

Thus, higher prestimulus alpha activity in S1 (but not VPL) led to a lower criterion for stimulus detection, resulting in more stimulus-present responses, regardless of actual stimulus presence. This supports the notion that prestimulus alpha activity in S1 influences decision making.

Discussion

In the current study, we explored the oscillatory dynamics in the somatosensory thalamocortical network in two monkeys performing a somatosensory detection task (5, 6). Most prominently, we observed a poststimulus, task-related sustained increase in beta power in VPL and a decrease in alpha power in S1. These oscillatory modulations appeared to depend on behavioral context, as they were stronger for the active detection than the passive control condition. Furthermore, the poststimulus theta power increase in both VPL and S1, and the alpha/beta band decrease in S1, reflected the outcome of the monkey's perceptual decision (stimulus-present vs. stimulus-absent), regardless of its accuracy. Additionally, we found that prestimulus alpha activity in S1 biased the behavioral response regardless of actual stimulus presence, with higher prestimulus alpha leading to a lower

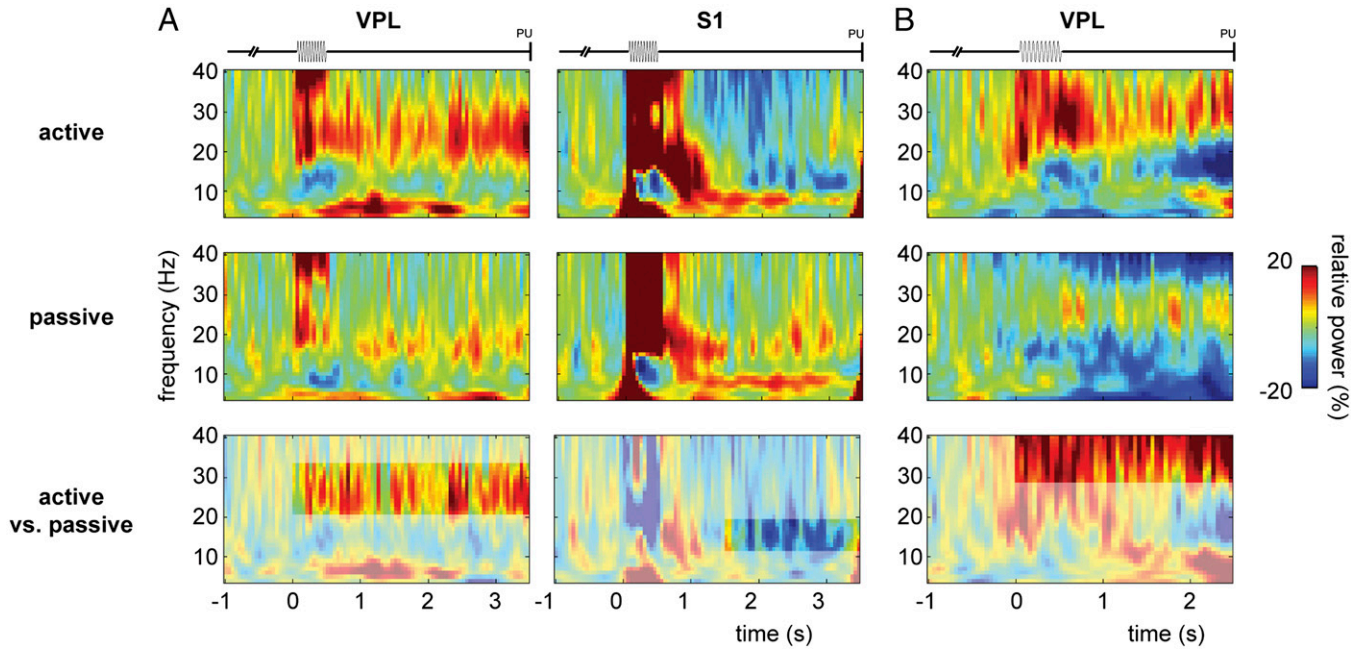

Fig. 5. Oscillatory activity during somatosensory detection task for the active vs. passive condition. (*A*) TFRs of power (4–40 Hz) for the active (*Top*) and (*Middle*) passive conditions for VPL (*Left*; $n = 21$ sites) and S1 (*Right*; $n = 35$ sites) in m26. (*Bottom*) Comparison between active vs. passive conditions, masked for significant results (cluster-corrected $P < 0.05$) based on a nonparametric randomization test. Trials were stratified such that both conditions contained the same number of trials per amplitude class. (*B*) Similar presentation for VPL in m27 ($n = 11$ sites). Note that for m27, the poststimulus window was shorter ($t = 0.5$–2.5 s).

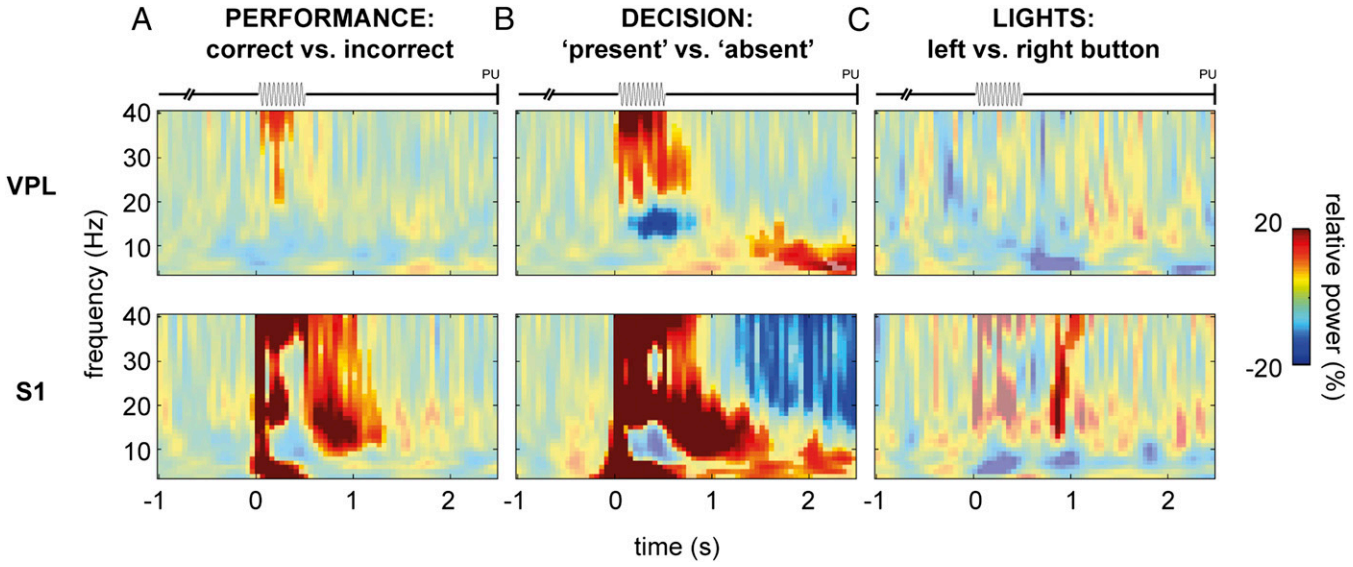

Fig. 6. Oscillatory activity during somatosensory detection task for behavioral contrasts. (*A*) TFRs of power (4–40 Hz) for the performance contrast, i.e., correct vs. incorrect responses, for VPL (*Upper*; $n = 58$ sites) and S1 (*Lower*; $n = 62$ sites). Note that here we combined the data for m26 and m27. Power is masked for significant results (cluster-corrected $P < 0.05$), based on a nonparametric randomization test of [hits and correct rejections] vs. [misses and false alarms]. (*B*) Similar presentation for the decision contrast, i.e., stimulus-present vs. stimulus-absent responses: [hits and false alarms] vs. [misses and correct rejections]. (*C*) Similar presentation for the lights control condition (VPL: $n = 29$ sites; S1: $n = 41$ sites), i.e., motor response contrast: left button vs. right button.

criterion for stimulus detection, resulting in more stimulus-present responses.

Studying the evoked response during the stimulus presentation, we found that both VPL and S1 LFPs reflected the stimulus frequency (20 Hz) and were modulated in power by the stimulus amplitude. This amplitude modulation was stronger in S1 than in VPL, which is in line with previous spike-firing rate results (16). This difference may be a result of the considerably smaller receptive field size in VPL than in S1 or of a gain amplification component, because S1 neurons receive converging input from several VPL neurons (27, 28). Furthermore, spike-field coherence showed a stronger interaction between VPL spikes and S1 fields, compared with coherence between S1 spikes and VPL fields, and also was modulated by stimulus amplitude, further suggesting the flow of stimulus information from thalamus to cortex.

Higher Prestimulus Alpha Power Reflects a More Liberal Strategy. Converging electrophysiological evidence suggests that the alpha rhythm plays an important functional role in sensory and cognitive processing. According to this view, decreased alpha activity facilitates processing, whereas increased alpha activity has a suppressing or inhibitory effect (29–31). In support of this view, several studies on somatosensory perception showed that anticipatory alpha activity reflects the direction of attention and motor preparation and influences detection performance (2, 22, 23, 32–34).

Generally, these previous studies show that lower (prestimulus) alpha in attended or task-relevant regions, and higher alpha in to-be-ignored or task-irrelevant regions, leads to better performance. At first sight, our finding of higher prestimulus alpha power leading to more detection responses might seem at odds with the alpha-inhibition hypothesis. However, in our case, a higher probability of stimulus-present responses does not necessarily reflect better performance, as both hits and false alarms increase. Indeed, we found that d′ did not change significantly, i.e., discriminability remained the same, whereas the criterion decreased with higher prestimulus alpha. In other words, with higher prestimulus alpha power, the monkey applied a more liberal criterion level, and the responses became sloppier: more hits but at the cost of more false alarms.

One crucial difference between our paradigm and the aforementioned attention studies is that in our task, half the trials were stimulus-absent, and of the stimulus-present trials, a substantial part was subthreshold. The monkeys were rewarded for both hits and correct rejections. Hence, this may lead to a strategy different from that of a task with 100% stimulus presence. Perhaps here, low prestimulus alpha reflects a focused, attentive

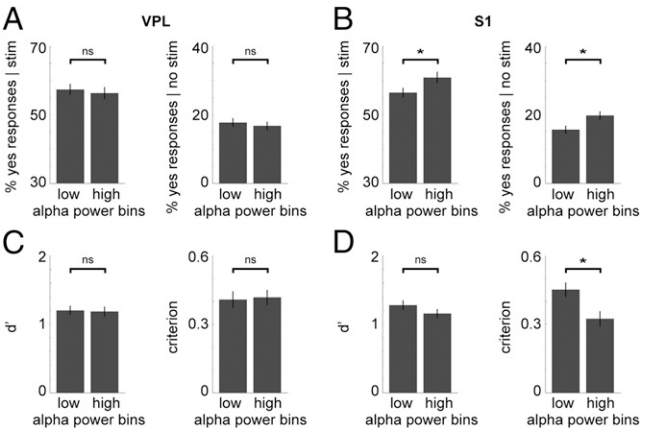

Fig. 7. Prestimulus alpha power in S1 influences detection performance: 10-pulse task. (*A*) Bar graphs showing no significant difference in performance between trials with low and those with high prestimulus alpha power in VPL ($n = 58$ sites), for both stimulus-present (*Left*) and stimulus-absent (*Right*) trials. Error bars indicate the SEM. (*B*) Similar graphs for S1 ($n = 62$ sites), showing a significant difference in performance. Higher prestimulus alpha power increased the probability of a yes response, for both stimulus-present ($P < 0.05$) and stimulus-absent trials ($P < 0.01$). (*C*) Bar graphs showing the d′ and criterion for low vs. high prestimulus alpha trials in VPL. There was no significant difference in the d′ or criterion. (*D*) Similar graphs for S1. There was no significant difference in the d′, whereas the criterion was significantly lower for high prestimulus alpha trials ($P < 0.01$).

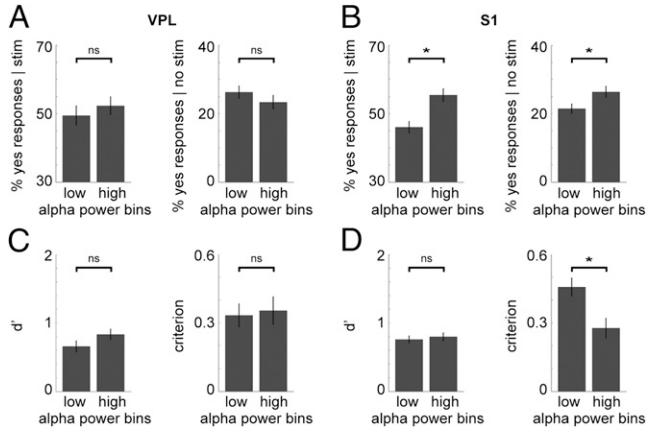

Fig. 8. Prestimulus alpha power in S1 influences detection performance: one-pulse task. (*A*) Bar graphs showing no significant difference in performance between trials with low and those with high prestimulus alpha power in VPL ($n = 26$ sites), for both stimulus-present (*Left*) and stimulus-absent (*Right*) trials, for the one-pulse experiment. Error bars indicate the SEM. (*B*) Similar graphs for S1 ($n = 43$ sites), showing a significant difference in performance. Higher prestimulus alpha power increased the probability of a yes response, for both stimulus-present ($P < 0.001$) and stimulus-absent trials ($P < 0.05$). (*C*) Bar graphs showing the d′ and criterion for low vs. high prestimulus alpha trials in VPL. There was no significant difference in the d′ or the criterion. (*D*) Similar graphs for S1. There was no significant difference in the d′, whereas the criterion was significantly lower for high prestimulus alpha trials ($P < 0.001$).

state in which the monkey was more careful and conservative in responding, whereas high prestimulus alpha reflects a less vigilant state in which the monkey adopted a more liberal strategy, which maintained overall performance by increasing the hit rate but at the cost of more false alarms. In future research, it would be interesting to determine whether introducing an attention manipulation or different reward schemes that change the optimal strategy leads to changes in the observed relation between alpha and performance.

Furthermore, it would be interesting to see the oscillatory patterns in the extended sensorimotor network. Here, we focused on S1 contralateral to stimulation, but what happens in the ipsilateral S1? Based on previous studies, one might expect alpha power modulation in the opposite direction, i.e., an alpha increase to suppress interference. Similarly, a focal decrease and "surround" increase in alpha have been described for the motor system during movement (35). Additionally, premotor and motor areas are involved in the decision phase (9), during which an alpha decrease and additional beta modulation would be expected (36, 37).

Oscillatory Response Reflects Behavioral Relevance and Decision Outcome. The observed poststimulus alpha and beta band modulations were stronger for the active than the passive condition, supporting their task relevance. In addition, a poststimulus theta increase in both regions, and an alpha/beta decrease in S1, reflected the outcome of the monkey's perceptual decision (but not the motor response). These oscillatory observations are in line with earlier findings on somatosensory decision making (36–38). The lower alpha in S1 for active detection is congruent with the idea that decreased alpha reflects the engagement of a region, whereas the beta increase in VPL fits with the view of beta as a prominent sensorimotor rhythm reflecting active processing (but see below for a discussion on the role of beta). Because these task- and decision-related LFP modulations in both VPL and S1 were observed in the poststimulus window, it is possible that they reflect feedback from higher-order regions (27) regarding the decision outcome. Furthermore, the different oscillatory patterns in active vs. passive conditions might reflect an increase in attention with behavioral relevance, perhaps through top-down gain modulation of the thalamocortical network.

Previous studies using spike recordings in the VPM (15) and VPL (14) found no evidence of attentional modulation of firing rate. In the current experiment, VPL single-neuron firing rate modulation did not predict the animal's decision report (6), nor was there a difference in sensitivity to changes in the stimulus amplitude for the active vs. passive conditions (6, 39). Only a few thalamic LFP recordings (in first-order nuclei) in awake, behaving animals are reported in the literature. Previous recordings in the LGN, the visual equivalent of VPL, have revealed alpha/beta band modulations related to task context (17) and attention (40). In this context, it also has been shown that the modulation of alpha rhythms depends on the activity of neuronal populations in the pulvinar nucleus of the thalamus, related to the attentional state of a behaving monkey (41). Furthermore, functional MRI reports show attentional modulation of LGN activity (42–44), as well as LGN activity reflecting the subject's reported percept (45, 46). Also, a study in S1 showed blood oxygen level dependent modulations coinciding with low-frequency oscillatory activity, in the absence of firing-rate effects (47).

Although these studies examined different paradigms and modalities, they all suggest modulation of oscillatory activity in the absence of spike modulation, which is in line with our current findings. The study of oscillatory activity offers a view that is complementary to what is known from spike recordings, because the oscillations reflect neuronal population dynamics, indicating the state of a network, rather than single-cell responses. We propose that oscillatory activity in the early somatosensory thalamocortical network is modulated by task context, potentially through top-down attentional modulation and/or feedback processes from higher-order areas.

The Role of Somatosensory Beta Oscillations in Cognition. Interestingly, in S1, we observed a beta decrease (in addition to a prominent alpha decrease), whereas in VPL, there was a strong sustained beta increase. What causes this dissociation between beta patterns in these two regions? Beta traditionally is reported as a prominent sensorimotor rhythm (48); however, with regard to its functional role, the beta story is less clear-cut (49). It has been proposed that beta facilitates long-range interactions (50), plays an active role in perceptual decision making (51), and reflects the status quo (52), or rather cortical idling or deactivation (53, 54). Some authors divide the beta band into a low (~15 Hz) and a high beta range (20–30 Hz), each of which may have distinct functional roles (55, 56). Indeed, sometimes beta co-occurs with alpha activity (57), e.g., decreasing with somatosensory attention and stimulation (23, 58, 59), whereas in other cases, alpha and beta show a dissociation (22, 60), with beta activity behaving in ways more similar to a "low gamma" rhythm, reflecting task aspects (36, 61).

Thus, beta band rhythms seem to play more versatile roles, behaving either more alpha-like, decreasing during active engagement of a region, or more gamma-like, increasing with engagement. These rhythms might operate on overlapping frequency ranges. It might be that here, with the dissociated patterns of S1 beta decrease and VPL increase, we are tapping into these different beta rhythms. In this interpretation, the beta decrease in S1 is associated with the alpha decrease, reflecting attention/engagement, whereas the beta increase in VPL reflects activity perhaps related to top-down/feedback processes regarding decision and motor preparation. In this context, it is interesting to note that the beta rhythms observed in VPL and S1 spanned different frequency ranges.

To our knowledge, this is one of the first studies reporting concurrent LFP recordings in VPL and S1 of an awake, behaving animal. We show task-related modulations in theta, alpha, and

beta band oscillations, not only in the neocortex but also in the thalamus, reflecting the perceptual decision process and subsequent behavioral response. This suggests that these early sensory regions, in addition to their sensory functions, also may be actively involved in perceptual decision making, as shown here.

Methods

General. Two monkeys (*M. mulatta*), referred to as m26 and m27, were trained to perform a somatosensory detection task (Fig. 1) in which they had to detect a vibrotactile stimulus delivered to the right hand (5, 6). Both spikes and LFPs were recorded simultaneously from VPL and S1. Animals were handled in accordance with the standards of the National Institutes of Health and the Society for Neuroscience.

Experimental Paradigm. Vibrotactile stimuli were delivered to one fingertip of the monkey's restrained right hand. Stimuli consisted of a sinusoidal wave lasting 500 ms at 20 Hz (10 pulses) with amplitudes varying from sub- to suprathreshold values (1–34 μm). Half the trials contained a stimulus (stimulus-present trials) and the other half contained no stimulus (stimulus-absent trials). At least 10 repetitions for each stimulus-amplitude were presented and counterbalanced with the same number of stimulus-absent trials. Trials were presented randomly. A trial began when the stimulator probe indented the skin of one fingertip of the restrained right hand, upon which the monkey placed its free left hand on an immovable key. After a variable prestimulus period (1.5–3 s), a vibrotactile stimulus could be presented or not (0.5 s). After a fixed delay (3 s for m26, 2 s for m27), the stimulator probe went up, which was the go-cue indicating to the monkey that it could report its perception by pressing one of two buttons with its free hand. Note that the probe was covered and movements of the probe were not visible to the monkey. A left button was used to indicate stimulus presence and a right button for absence. The design of the task elicited four different behavioral responses: hits and misses for stimulus-present trials and correct rejections and false alarms for stimulus-absent trials. The animal was rewarded for correct responses by a drop of liquid.

In addition to the experimental condition, the animals also performed two control conditions: (*i*) a passive control task (passive condition) during which the same stimuli were presented but no response was required, and (*ii*) a motor control task (lights condition) during which a light presented during the entire trial indicated which button was to be pressed, independent of the stimulus (6). Thus, during the passive condition, sensory information entered the system but the animal was not forced to use it to get a reward, and during the lights condition, sensory input and motor output were the same as during the experimental condition, but no perceptual decision process was involved. Furthermore, one monkey (m26) performed an additional experimental condition in which the pulse-train stimulus was replaced by a single sinusoidal pulse lasting 50 ms (referred to as the one-pulse experiment).

Data Acquisition. Neuronal recordings were obtained by using two arrays, each with seven independent, movable microelectrodes (2–3 MΩ; see refs. 62, 63). Arrays were located in S1, one in the cutaneous representation of the fingers (area 1 and 3b) and the other medial to the hand's representation in a way that allowed us to lower the microelectrodes to the VPL of the somatosensory thalamus. Recordings were performed contralateral to the stimulated hand and ipsilateral to the responding one. Areas were identified using cortical landmarks based on a standard atlas. Each recording began with a mapping session to find the cutaneous representation of the fingers in VPL. Subsequently, we mapped neurons in S1 (area 1 and 3b) sharing receptive fields with the neurons of VPL. All recorded neurons had small cutaneous receptive fields with quickly or slowly adapting properties. Locations of the electrode penetrations in VPL and S1 were confirmed with standard histological techniques.

The neuronal signal of each microelectrode was sampled at 30 kHz and spikes were sorted online. Simultaneously, the LFPs were obtained using a 250 Hz low-pass filter and stored at 2 kHz for offline analysis. A more extensive description of the task and recording procedure can be found in previous publications (5, 6, 63).

Here, we report data from multiple recording sessions during which LFPs were obtained from two animals, m26 and m27. For the experimental condition, we recorded 42 sessions with 120–140 trials per session in m26 (38 sites in VPL, 59 in S1) and 21 sessions with up to 360 trials in m27 [20 sites in VPL, 3 in S1 (included only in the analysis for Figs. 6 and 7, in which data from the two monkeys were combined, and for the amplitude modulation analysis)]. For the one-pulse experimental condition in m26, we obtained 29 sessions with 120–140 trials (26 sites in VPL, 43 in S1). For the passive control condition, we obtained 24 sessions with 70–140 trials in m26 (21 sites in VPL, 35 in S1) and 11 sessions with 70–210 trials in m27 (11 sites in VPL). For the lights control condition, we obtained 29 sessions with 80 trials in m26 (26 sites in VPL, 41 sites in S1) and 3 sessions with 120 trials in m27 (3 sites in VPL).

Behavioral Analysis. Performance was computed in terms of the four response categories, i.e., hit and miss rates for stimulus-present trials and correct rejection and false alarm rates for stimulus-absent trials. Furthermore, using signal detection theory, the d′ and the criterion for signal detection were computed as follows (64):

$$d' = z(\text{hit rate}) - z(\text{false alarm rate}) \quad [1]$$

$$\text{criterion} = -[z(\text{hit rate}) + z(\text{false alarm rate})]/2 \quad [2]$$

with z the statistical standard z score.

Data Analysis. We used custom-built MATLAB code and the FieldTrip toolbox (65) to analyze the data. The data were down-sampled offline to a sampling frequency of 1 kHz. A band-stop filter was applied to remove line noise caused by the power net (60 Hz and harmonics). Trials containing artifacts (e.g., due to movement or electronic interference) were removed based on visual inspection of the data.

Spectral Analysis. Using a fast Fourier transform approach, we computed TFRs of power (4–40 Hz) using an adaptive sliding time window four cycles long ($\Delta t = 4/f$) multiplied with a Hanning taper. Per condition of interest, the TFRs were averaged over trials within each recording session and normalized by a relative baseline correction ($t = -1 - -0.5$). This procedure gave the average TFRs per recording site for each session, which was used in the statistical analysis. Subsequently, a grand average was computed over recording sites (per region) for visualization purposes.

Furthermore, for specific time windows of interest (prestimulus and stimulus window), we computed the power spectra (4–40 Hz). Trials were segmented into epochs (1 s prestimulus, 0.5 s during stimulus presentation) and multiplied with a Hanning taper to improve the spectral estimation. These spectra were used to compute the amplitude modulation and the relation between prestimulus alpha and performance (*Results*).

SFC was calculated by using the spectra $S_x(f)$ and $S_y(f)$ of the fields and spikes, respectively, and their cross-spectrum, $S_{yx}(f)$, in the following equation:

$$C_{yx}(f) = \left|S_{yx}(f)/\sqrt{(S_x(f)S_y(f))}\right|. \quad [3]$$

SFC quantifies synchronization between two signals, i.e., the constant phase relationship (and amplitude covariation), and ranges between 0, indicating no relationship, and 1, indicating that the two signals are fully coherent (66).

Statistical Analysis. We applied a cluster-based nonparametric randomization test (67) to establish whether the differences in power between two conditions as observed in the TFRs (i.e., task vs. baseline activation, experimental vs. control condition) were significantly different from 0. By clustering neighboring samples (i.e., time-frequency points) that show the same effect, this test deals with the multiple-comparisons problem while accounting for the dependency of the data. For each sample, a dependent sample t-value was computed. All samples for which this t-value exceeded an a priori threshold (uncorrected $P < 0.05$) were selected and subsequently clustered on the basis of temporal–spectral adjacency. The sum of the t-values within a cluster was used as the cluster-level statistic, and the cluster with the maximum sum then was used as the test statistic. This was computed within recording sites (separately per region). By randomizing the data across the two conditions and recalculating the test statistic 2,000 times, we obtained a reference distribution of maximum cluster t-values to evaluate the statistics of the actual data.

ACKNOWLEDGMENTS. The authors thank Lucia Melloni for insightful feedback on the manuscript. S.H. was supported by Rubicon Grant 446.11.009 from The Netherlands Organization for Scientific Research; O.J. was supported by Vici Grant 453.09.002 from The Netherlands Organization for Scientific Research and Netherlands Initiative for Brain and Cognition "The healthy brain" scheme (056-14-011); R.R. was supported by an International Research Scholars Award from the Howard Hughes Medical Institute and by grants from the Consejo Nacional de Ciencia y Tecnología and Dirección del Personal Académico de la Universidad Nacional Autónoma de México.

1. Libet B, Alberts WW, Wright EW, Jr., Feinstein B (1967) Responses of human somatosensory cortex to stimuli below threshold for conscious sensation. *Science* 158(3808):1597–1600.
2. Haegens S, Händel BF, Jensen O (2011) Top-down controlled alpha band activity in somatosensory areas determines behavioral performance in a discrimination task. *J Neurosci* 31(14):5197–5204.
3. Linkenkaer-Hansen K, Nikulin VV, Palva S, Ilmoniemi RJ, Palva JM (2004) Prestimulus oscillations enhance psychophysical performance in humans. *J Neurosci* 24(45): 10186–10190.
4. Zhang Y, Ding M (2010) Detection of a weak somatosensory stimulus: Role of the prestimulus mu rhythm and its top-down modulation. *J Cogn Neurosci* 22(2):307–322.
5. de Lafuente V, Romo R (2005) Neuronal correlates of subjective sensory experience. *Nat Neurosci* 8(12):1698–1703.
6. Vázquez Y, Zainos A, Alvarez M, Salinas E, Romo R (2012) Neural coding and perceptual detection in the primate somatosensory thalamus. *Proc Natl Acad Sci USA* 109(37):15006–15011.
7. Romo R, Salinas E (2003) Flutter discrimination: neural codes, perception, memory and decision making. *Nat Rev Neurosci* 4(3):203–218.
8. Romo R, de Lafuente V (2013) Conversion of sensory signals into perceptual decisions. *Prog Neurobiol* 103:41–75.
9. de Lafuente V, Romo R (2006) Neural correlate of subjective sensory experience gradually builds up across cortical areas. *Proc Natl Acad Sci USA* 103(39):14266–14271.
10. Viaene AN, Petrof I, Sherman SM (2011) Synaptic properties of thalamic input to the subgranular layers of primary somatosensory and auditory cortices in the mouse. *J Neurosci* 31(36):12738–12747.
11. Viaene AN, Petrof I, Sherman SM (2011) Synaptic properties of thalamic input to layers 2/3 and 4 of primary somatosensory and auditory cortices. *J Neurophysiol* 105(1):279–292.
12. Johnson MJ, Alloway KD (1996) Cross-correlation analysis reveals laminar differences in thalamocortical interactions in the somatosensory system. *J Neurophysiol* 75(4): 1444–1457.
13. Temereanca S, Brown EN, Simons DJ (2008) Rapid changes in thalamic firing synchrony during repetitive whisker stimulation. *J Neurosci* 28(44):11153–11164.
14. Poranen A, Hyvärinen J (1982) Effects of attention on multiunit responses to vibration in the somatosensory regions of the monkey's brain. *Electroencephalogr Clin Neurophysiol* 53(5):525–537.
15. Tremblay N, Bushnell MC, Duncan GH (1993) Thalamic VPM nucleus in the behaving monkey. II. Response to air-puff stimulation during discrimination and attention tasks. *J Neurophysiol* 69(3):753–763.
16. Vázquez Y, Salinas E, Romo R (2013) Transformation of the neural code for tactile detection from thalamus to cortex. *Proc Natl Acad Sci USA* 110(28):E2635–E2644.
17. Wilke M, Mueller K-M, Leopold DA (2009) Neural activity in the visual thalamus reflects perceptual suppression. *Proc Natl Acad Sci USA* 106(23):9465–9470.
18. Lehky SR, Maunsell JHR (1996) No binocular rivalry in the LGN of alert macaque monkeys. *Vision Res* 36(9):1225–1234.
19. McAlonan K, Cavanaugh J, Wurtz RH (2008) Guarding the gateway to cortex with attention in visual thalamus. *Nature* 456(7220):391–394.
20. Palva S, Linkenkaer-Hansen K, Näätänen R, Palva JM (2005) Early neural correlates of conscious somatosensory perception. *J Neurosci* 25(21):5248–5258.
21. Monto S, Palva S, Voipio J, Palva JM (2008) Very slow EEG fluctuations predict the dynamics of stimulus detection and oscillation amplitudes in humans. *J Neurosci* 28(33):8268–8272.
22. Haegens S, Luther L, Jensen O (2012) Somatosensory anticipatory alpha activity increases to suppress distracting input. *J Cogn Neurosci* 24(3):677–685.
23. Jones SR, et al. (2010) Cued spatial attention drives functionally relevant modulation of the mu rhythm in primary somatosensory cortex. *J Neurosci* 30(41):13760–13765.
24. Schubert R, Haufe S, Blankenburg F, Villringer A, Curio G (2009) Now you'll feel it, now you won't: EEG rhythms predict the effectiveness of perceptual masking. *J Cogn Neurosci* 21(12):2407–2419.
25. van Ede F, Köster M, Maris E (2012) Beyond establishing involvement: Quantifying the contribution of anticipatory α- and β-band suppression to perceptual improvement with attention. *J Neurophysiol* 108(9):2352–2362.
26. Lange J, Halacz J, van Dijk H, Kahlbrock N, Schnitzler A (2012) Fluctuations of prestimulus oscillatory power predict subjective perception of tactile simultaneity. *Cereb Cortex* 22(11):2564–2574.
27. Sherman SM, Guillery RW (2011) Distinct functions for direct and transthalamic corticocortical connections. *J Neurophysiol* 106(3):1068–1077.
28. Bruno RM, Sakmann B (2006) Cortex is driven by weak but synchronously active thalamocortical synapses. *Science* 312(5780):1622–1627.
29. Cooper NR, Croft RJ, Dominey SJJ, Burgess AP, Gruzelier JH (2003) Paradox lost? Exploring the role of alpha oscillations during externally vs. internally directed attention and the implications for idling and inhibition hypotheses. *Int J Psychophysiol* 47(1): 65–74.
30. Jensen O, Mazaheri A (2010) Shaping functional architecture by oscillatory alpha activity: Gating by inhibition. *Front Hum Neurosci* 4:186.
31. Klimesch W, Sauseng P, Hanslmayr S (2007) EEG alpha oscillations: The inhibition-timing hypothesis. *Brain Res Brain Res Rev* 53(1):63–88.
32. Anderson KL, Ding M (2011) Attentional modulation of the somatosensory mu rhythm. *Neuroscience* 180:165–180.
33. van Ede F, de Lange F, Jensen O, Maris E (2011) Orienting attention to an upcoming tactile event involves a spatially and temporally specific modulation of sensorimotor alpha- and beta-band oscillations. *J Neurosci* 31(6):2016–2024.
34. Haegens S, Osipova D, Oostenveld R, Jensen O (2010) Somatosensory working memory performance in humans depends on both engagement and disengagement of regions in a distributed network. *Hum Brain Mapp* 31(1):26–35.
35. Lopes da Silva F (2013) EEG and MEG: Relevance to neuroscience. *Neuron* 80(5): 1112–1128.
36. Haegens S, et al. (2011) Beta oscillations in the monkey sensorimotor network reflect somatosensory decision making. *Proc Natl Acad Sci USA* 108(26):10708–10713.
37. Haegens S, Nácher V, Luna R, Romo R, Jensen O (2011) α-Oscillations in the monkey sensorimotor network influence discrimination performance by rhythmical inhibition of neuronal spiking. *Proc Natl Acad Sci USA* 108(48):19377–19382.
38. Spitzer B, Blankenburg F (2011) Stimulus-dependent EEG activity reflects internal updating of tactile working memory in humans. *Proc Natl Acad Sci USA* 108(20): 8444–8449.
39. Camarillo L, Luna R, Nácher V, Romo R (2012) Coding perceptual discrimination in the somatosensory thalamus. *Proc Natl Acad Sci USA* 109(51):21093–21098.
40. Wróbel A, Bekisz M, Kublik E, Waleszczyk W (1994) 20 Hz bursting beta activity in the cortico-thalamic system of visually attending cats. *Acta Neurobiol Exp (Warsz)* 54(2): 95–107.
41. Saalmann YB, Pinsk MA, Wang L, Li X, Kastner S (2012) The pulvinar regulates information transmission between cortical areas based on attention demands. *Science* 337(6095):753–756.
42. Saalmann YB, Kastner S (2011) Cognitive and perceptual functions of the visual thalamus. *Neuron* 71(2):209–223.
43. Schneider KA, Kastner S (2009) Effects of sustained spatial attention in the human lateral geniculate nucleus and superior colliculus. *J Neurosci* 29(6):1784–1795.
44. O'Connor DH, Fukui MM, Pinsk MA, Kastner S (2002) Attention modulates responses in the human lateral geniculate nucleus. *Nat Neurosci* 5(11):1203–1209.
45. Haynes J-D, Deichmann R, Rees G (2005) Eye-specific effects of binocular rivalry in the human lateral geniculate nucleus. *Nature* 438(7067):496–499.
46. Wunderlich K, Schneider KA, Kastner S (2005) Neural correlates of binocular rivalry in the human lateral geniculate nucleus. *Nat Neurosci* 8(11):1595–1602.
47. Maier A, et al. (2008) Divergence of fMRI and neural signals in V1 during perceptual suppression in the awake monkey. *Nat Neurosci* 11(10):1193–1200.
48. Pfurtscheller G, Lopes da Silva FH (1999) Event-related EEG/MEG synchronization and desynchronization: basic principles. *Clin Neurophysiol* 110(11):1842–1857.
49. Kilavik BE, Zaepffel M, Brovelli A, MacKay WA, Riehle A (2013) The ups and downs of β oscillations in sensorimotor cortex. *Exp Neurol* 245(0):15–26.
50. Varela F, Lachaux J-P, Rodriguez E, Martinerie J (2001) The brainweb: Phase synchronization and large-scale integration. *Nat Rev Neurosci* 2(4):229–239.
51. Siegel M, Engel AK, Donner TH (2011) Cortical network dynamics of perceptual decision-making in the human brain. *Front Hum Neurosci* 5:21.
52. Engel AK, Fries P (2010) Beta-band oscillations—signalling the status quo? *Curr Opin Neurobiol* 20(2):156–165.
53. Pfurtscheller G, Stancák A, Jr., Neuper C (1996) Event-related synchronization (ERS) in the alpha band—an electrophysiological correlate of cortical idling: a review. *Int J Psychophysiol* 24(1-2):39–46.
54. Neuper C, Pfurtscheller G (2001) Event-related dynamics of cortical rhythms: Frequency-specific features and functional correlates. *Int J Psychophysiol* 43(1):41–58.
55. Kopell N, Whittington MA, Kramer MA (2011) Neuronal assembly dynamics in the beta1 frequency range permits short-term memory. *Proc Natl Acad Sci USA* 108(9): 3779–3784.
56. Roopun AK, et al. (2006) A beta2-frequency (20-30 Hz) oscillation in nonsynaptic networks of somatosensory cortex. *Proc Natl Acad Sci USA* 103(42):15646–15650.
57. Jones SR, et al. (2009) Quantitative analysis and biophysically realistic neural modeling of the MEG mu rhythm: Rhythmogenesis and modulation of sensory-evoked responses. *J Neurophysiol* 102(6):3554–3572.
58. Bauer M, Oostenveld R, Peeters M, Fries P (2006) Tactile spatial attention enhances gamma-band activity in somatosensory cortex and reduces low-frequency activity in parieto-occipital areas. *J Neurosci* 26(2):490–501.
59. van Ede F, Jensen O, Maris E (2010) Tactile expectation modulates pre-stimulus beta-band oscillations in human sensorimotor cortex. *Neuroimage* 51(2):867–876.
60. Ray WJ, Cole HW (1985) EEG alpha activity reflects attentional demands, and beta activity reflects emotional and cognitive processes. *Science* 228(4700):750–752.
61. Spitzer B, Wacker E, Blankenburg F (2010) Oscillatory correlates of vibrotactile frequency processing in human working memory. *J Neurosci* 30(12):4496–4502.
62. Romo R, Brody CD, Hernández A, Lemus L (1999) Neuronal correlates of parametric working memory in the prefrontal cortex. *Nature* 399(6735):470–473.
63. Hernández A, et al. (2008) Procedure for recording the simultaneous activity of single neurons distributed across cortical areas during sensory discrimination. *Proc Natl Acad Sci USA* 105(43):16785–16790.
64. Stanislaw H, Todorov N (1999) Calculation of signal detection theory measures. *Behav Res Methods Instrum Comput* 31(1):137–149.
65. Oostenveld R, Fries P, Maris E, Schoffelen J-M (2011) FieldTrip: Open source software for advanced analysis of MEG, EEG, and invasive electrophysiological data. *Comput Intell Neurosci* 2011(156869):156869.
66. Fries P, Womelsdorf T, Oostenveld R, Desimone R (2008) The effects of visual stimulation and selective visual attention on rhythmic neuronal synchronization in macaque area V4. *J Neurosci* 28(18):4823–4835.
67. Maris E, Oostenveld R (2007) Nonparametric statistical testing of EEG- and MEG-data. *J Neurosci Methods* 164(1):177–190.